Azimuthal 2α correlations and projectile-residue distributions selected by neutron and charged-particle multiplicity measurements

G. J. Kunde, S. Gaff, C. K. Gelbke, T. Glasmacher, M. J. Huang, R. Lemmon, W. G. Lynch, L. Manduci, L. Martin, R. Popescu, and M. B. Tsang
Department of Physics and Astronomy and National Superconducting Cyclotron Laboratory, Michigan State University, East Lansing, Michigan 48824

J. Dempsey, R. J. Charity, and L. G. Sobotka
Department of Chemistry, Washington University, St. Louis, Missouri 63130

D. K. Agnihotri, B. Djerroud, W. U. Schröder, W. Skulski, J. Tõke, and K. Wyrozebski
Department of Chemistry and Nuclear Structure Research Laboratory, University of Rochester, Rochester, New York 14627

D. Ruess
Department of Chemistry, University of Maryland, College Park, Maryland 20742
(Received 23 April 1996)

The resolution of reaction filters for intermediate-energy heavy-ion collisions based upon charged-particle and neutron multiplicity measurements with 4π coverage is compared for ^{112}Sn+^{112}Sn and ^{124}Sn+^{124}Sn collisions at $E/A=40$ MeV. The quality of event characterization is inferred from the azimuthal correlations of α particles emitted at intermediate rapidity and from the Z distributions of projectilelike fragments emitted at forward angles. For central and midimpact parameter collisions, the associated charged-particle multiplicity appears to provide better impact-parameter selection than the associated neutron multiplicity. [S0556-2813(97)50203-2]

PACS number(s): 25.70.Pq, 25.70.Gh

For energetic nucleus-nucleus collisions, many experimental observables are predicted to exhibit a strong dependence upon impact parameter [1]. Reaction models are therefore most sensitively tested by ''exclusive'' experiments which provide reaction filters capable of selecting events according to narrow ranges of impact parameters. For intermediate-energy nucleus-nucleus collisions, such a selection is often obtained from the multiplicity of emitted neutrons [2] or charged particles [3]. Only limited information about the relative selectivity of various reaction filters is available [4–9], and no quantitative comparison of neutron and charged-particle multiplicity filters exists.

A number of examples underline the importance of a comparison of event selection based upon neutron and charged-particle multiplicity measurements. Very similar neutron multiplicity (N_N) distributions were observed in Ar+Au (and Th) collisions at $E/A=44$ and 77 MeV [10]. However, over the energy range $E/A=35$–110 MeV, the multiplicity distribution of charged particles (N_C) was observed to extend to higher values of N_C with increasing beam energy [11]. Collisions of ^{136}Xe+^{209}Bi at $E/A=28$ MeV, selected by cuts [12] on high neutron ($N_N \geqslant 29$) or charged-particle multiplicities ($N_C \geqslant 18$) or by a two-dimensional cut on both ($N_N>22$, $N_C>9$) [13], indicated the survival of a target and projectilelike source [12,13]. In these measurements, fragment emission occurred predominantly from the breakup of a ''neck zone'' situated intermediately between the two heavy residues [13]. On the other hand, collisions of ^{197}Au+^{197}Au at $E/A=35$ MeV, selected by a ''central'' cut on high charged-particle multiplicity ($N_C \geqslant 24$), indicated by predominantly isotropic fragment emission from a single, nearly equilibrated source [14,15]. A comparison between neutron and charged-particle multiplicity filters revealed higher multiplicities of intermediate mass fragments (IMF) when central Sn+Sn collisions were selected by cuts on N_C than when selected by cuts on N_N [16]. These observations raise the question [16] of whether the selection of small impact parameters by cuts on N_N provides a resolution comparable to that provided by cuts on N_C.

Examination of other observables with a strong impact parameter dependence, such as the azimuthal distribution of α particles emitted at intermediate rapidity [9] or the charge distribution of projectilelike fragments (PLF) emitted at small angles, can provide information about the relative resolution of the two reaction filters. These techniques are applied, for the first time, in this paper to evaluate the relative resolution of reaction filters based upon neutron and charged-particle multiplicity measurements.

The experiment was performed at the National Superconducting Cyclotron Laboratory at Michigan State University. To optimize the relationship between impact parameter and emitted particle multiplicity, symmetric reactions were studied [1]. To explore the sensitivity to the N/Z ratio of projectile and target, we performed measurements for ^{112}Sn+^{112}Sn and ^{124}Sn+^{124}Sn, at a beam energy of $E/A=40$ MeV. The areal density of the targets was 5 mg/cm^2. For each event, the associated neutron multiplicity was measured with the SuperBall neutron multiplicity meter [17], the largest device of its kind currently available. The neutron-detection efficiency was estimated [17] to be approximately 80% for emission from a targetlike source, 50% for emission from a projectilelike source, and 65% on average. Coincident charged par-

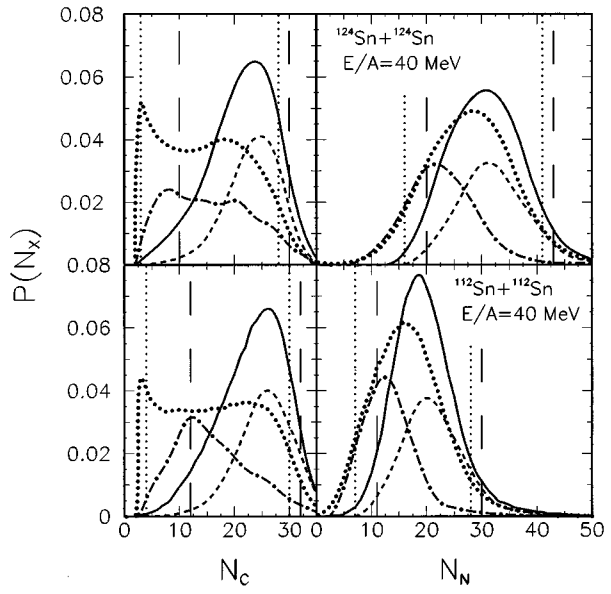

FIG. 1. Charged-particle (N_C, left panels) and neutron (N_N, right panels) multiplicity distributions measured for the event trigger (dotted curves) and with the additional requirement of detecting two coincident α particles at $25° \leqslant \theta_{lab} \leqslant 60°$ (solid curves). Top and bottom panels show results for ^{124}Sn+^{124}Sn and ^{112}Sn+^{112}Sn, respectively. The 2α-coincidence requirement at $25° \leqslant \theta_{lab} \leqslant 60°$ reduces the trigger yield by a factor of three, but for ease of presentation the two curves were normalized to unit area. The left (right) long-dashed vertical lines delimit the upper (lower) multiplicity boundaries for the peripheral (central) collision gates which delimit the lower (upper) 5% of the areas under the solid curves. The dotted vertical lines show analogous 5% cuts for the dotted curves which represent the event trigger without the 2α-coincidence requirement. The dot-dashed and dashed curves show N_C (N_N) distributions selected by the peripheral and central cuts on N_N (N_C) defined by the long-dashed vertical lines; for ease of presentation, these curves were normalized to subtend an area of 0.5.

ticles were measured with 280 plastic scintillator-CsI(TI) phoswich detectors of the Miniball/Miniwall array [18,19] mounted in the SuperBall scattering chamber [20]. The charged particle array covered approximately 90% of 4π. It provided isotopic resolution for H and He nuclei and elemental resolution for heavier fragments ($Z \leqslant 20$) with approximate energy thresholds of $E_{th}/A \approx 2.2$ MeV (4.5 MeV) for $Z=3$ ($Z=10$) particles detected in the Miniwall at $5.4° \leqslant \theta_{lab} \leqslant 25°$, and $E_{th}/A \approx 1.5$ MeV (2.5 MeV) for $Z=3$ ($Z=10$) particles detected in the Miniball at $25° \leqslant \theta_{lab} \leqslant 160°$, respectively. Projectilelike fragments with $Z \geqslant 15$ were detected in a Si-CsI(Tl) array (300 μm Si and 20 mm CsI) covering the angular range of $2.5 \leqslant \theta_{lab} \leqslant 5.4°$. The event trigger required the detection of at least two charged particles in the Miniball/Miniwall array.

Multiplicity distributions of detected charged particles (N_C) and neutrons (N_N) are shown in the left and right panels of Fig. 1; the top and bottom panels are for ^{124}Sn+^{124}Sn and ^{112}Sn+^{112}Sn. Dotted and solid curves show distributions measured in coincidence with the event trigger and in coincidence with two α particles detected at $25° \leqslant \theta_{lab} \leqslant 60°$. For ease of presentation, these two curves are normalized to unit area, even though the 2α-coincidence requirement at $25° \leqslant \theta_{lab} \leqslant 60°$ reduces the trigger yield by a factor of three. The event trigger suppresses low neutron-multiplicity events corresponding to the most peripheral collisions for which few charged particles are emitted. An additional, more significant suppression of peripheral events arises from the 2α-coincidence requirement (solid curves) needed for the construction of the azimuthal correlation functions discussed below. The left (right) long-dashed vertical lines delimit the upper (lower) multiplicity boundaries for the peripheral (central) collision gates which delimit the lower (upper) 5% of the areas under the solid curves. The dotted vertical lines show analogous 5% cuts for the event trigger (used in Fig. 4) without the 2α-coincidence requirement. The dashed and dot-dashed curves show the shapes of the N_N (N_C) distributions selected by central and peripheral cuts on N_C (N_N); for ease of presentation, these curves were normalized to subtend an area of 0.5. Narrow cuts on N_C produce rather broad distributions in N_N and vice versa—thus *corresponding cuts on N_C and N_N select different, though somewhat overlapping classes of events.*

In order to explore the selectivity of cuts on N_C and N_N, we investigate the shapes of azimuthal α-α correlation functions which have been shown to strongly correlate with various reaction filters [9]. For the reactions considered here, these correlations are dominated by a rotational motion which produces a characteristic ''V shape'' of the azimuthal correlation function [9,21–24]. The azimuthal α-α correlation functions are defined as

$$1 + R(\Delta\phi_{\alpha\alpha}) = \frac{\Sigma Y_{\alpha\alpha}(\theta_1, \phi_1, \theta_2, \phi_2)}{Y_{back}(\theta_1, \phi_1, \theta_2, \phi_2)} . \qquad (1)$$

Here $Y_{\alpha\alpha}(\theta_1, \phi_1, \theta_2, \phi_2)$ is the coincidence yield for the detection of two α particles at polar and azimuthal angles θ_i and $\phi_i (i=1,2)$ and $Y_{back}(\theta_1, \phi_1, \theta_2, \phi_2)$ denotes the ''background'' yield constructed by the event mixing technique [25]. The sum in Eq. (1) extends over all pairs of α particles within a given bin of $\Delta\phi_{\alpha\alpha} = |\phi_1 - \phi_2|$ (defined over the interval [0°, 180°]) and with $25° \leqslant \theta_{lab} \leqslant 60°$. The cut on θ_{lab} selects α particles emitted at approximately $90° \pm 30°$ in the center-of-mass system. To reduce possible many-body Coulomb distortions for particles emitted at very low energy and eliminate small-angle distortions from the decay of particle-unstable ^{8}Be nuclei, the summations were further constrained by $E_{\alpha,lab} > 40$ MeV and $E_{rel} > 250$ keV, where E_{rel} is the kinetic energy in the α-α center-of-momentum system [26].

Figure 2 shows α-α correlation functions, selected by the peripheral and central cuts on N_C and N_N defined in Fig. 1. Top and bottom panels show results for ^{124}Sn+^{124}Sn and ^{112}Sn+^{112}Sn. Consistent with previous results [9,23], much stronger V-shaped correlations are observed for peripheral than for central, violent collisions [27]. For peripheral ^{112}Sn+^{112}Sn collisions, the V shape of the α-α correlation function is *more pronounced* for the cut on N_C than on N_N, but for peripheral ^{124}Sn+^{124}Sn collisions, the two cuts produce very similar correlation functions. Since ^{124}Sn+^{124}Sn collisions are associated with higher neutron multiplicities, this qualitative difference between the two reactions could be due to a difference in impact-parameter resolution for the peripheral cuts on N_N. For ^{124}Sn+^{124}Sn, peripheral cuts on N_N and N_C appear to have comparable

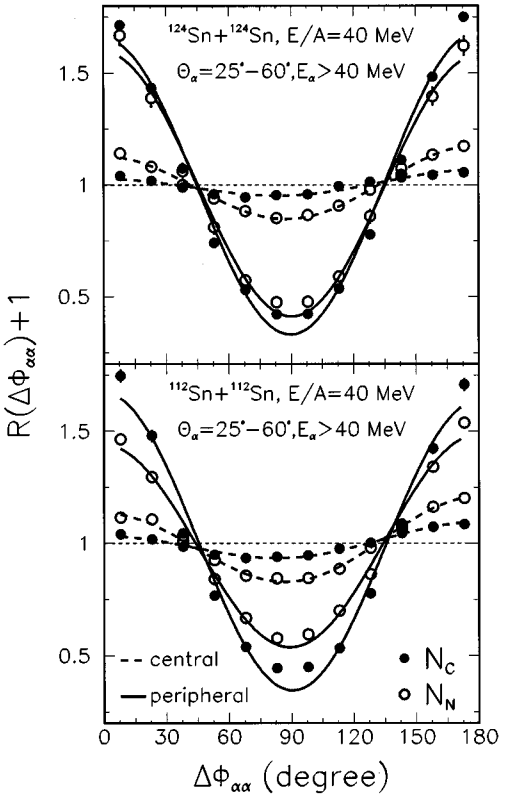

FIG. 2. Azimuthal α-α correlation functions observed for central and peripheral cuts on N_N (open points) and N_C (solid points). Top and bottom panels show results for ^{124}Sn+^{124}Sn and ^{112}Sn+^{112}Sn, respectively. Solid and dashed curves show fits [with Eq. (2)] to correlations selected by peripheral and central cuts, respectively.

resolution, but for the ^{112}Sn+^{112}Sn reaction cuts on N_C appear to provide better selectivity than cuts on N_N [28]. For both reactions, the α-α correlation functions are *more isotropic* for the central cut on N_C than on N_N.

For a more quantitative discussion [9], we have fitted the measured α-α correlation functions with the functional form [9,23,24]

$$1+R(\Delta\phi_{\alpha\alpha})=a_0(1+a_1\cos\Delta\phi_{\alpha\alpha}+a_2\cos 2\Delta\phi_{\alpha\alpha}), \quad (2)$$

where the parameters a_1 and a_2 provide a measure for sideward directed and rotational flow, respectively [24]. Representative fits are shown by the curves in Fig. 2 [29]. Parameters a_2 characterizing azimuthal α-α correlation functions selected by different cuts on N_C and N_N are shown in the left and right panels of Fig. 3 [29]. Open and solid points show the results for ^{112}Sn+^{112}Sn and ^{124}Sn+^{124}Sn, respectively. The reduced range of variation of a_2 for cuts on N_N (as compared to cuts on N_C) strongly suggests event selection with reduced resolution. The curves in the left (right) panels show the variation of a_2 as a function of N_C (N_N) when the events are further restricted by central cuts on N_N (N_C). Rather surprisingly, a central cut on N_N has little effect on the N_C dependence, but a central cut on N_C essentially defines a_2 with little further dependence on N_N. The

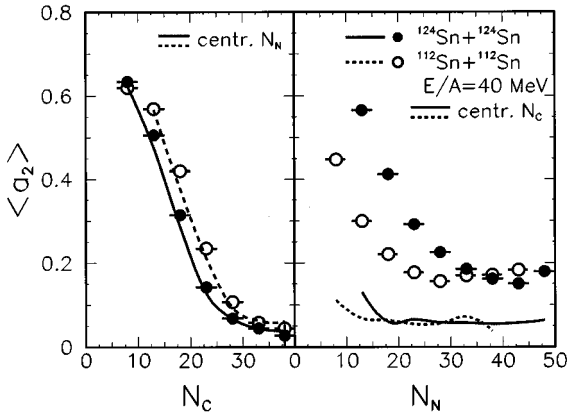

FIG. 3. Dependence of fit parameter a_2 [see Eq. (2)] on N_C and N_N. The curves show the dependences on N_C (N_N) for central collisions selected by a cut on N_N (N_C). Solid points and solid curves (open points and dashed curves) indicate results for ^{124}Sn+^{124}Sn (^{112}Sn+^{112}Sn).

shape of the azimuthal α-α correlation functions thus is well determined by cuts on N_C; additional constraints on N_N have little if any effect.

If one assumes that the shape of the α-α correlation function is primarily determined by the impact parameter of the collision [27]; then one is led to the conclusion that the impact parameter is better determined by cuts on N_C than on N_N and that, further, an additional cut on N_N does not improve the impact parameter selection. It is, however, conceivable that many-body Coulomb final-state interactions could attenuate the original emission pattern, thus leading to decreasing values of a_2 as a function of N_C, but not N_N, for a fixed impact parameter. While an accurate determination of final-state Coulomb distortions requires knowledge of the complete many-body emission function, we have estimated their possible importance via many-body Coulomb trajectory calculations [30], assuming an instantaneous release of all charged particles from the surface of a hot rotating gas, modeled as in Ref. [21]. Specifically, we used a realistic element distribution and source parameters [21], $(R\omega/c,T)=(0.08, 10$ MeV) and (0.1, 5 MeV), adjusted to provide an approximate description of the average α-particle energy spectrum and to produce azimuthal α-α correlations comparable to those measured. For simplicity, all particles were treated as point particles moving under the influence of their mutual Coulomb forces. This ansatz is likely to overestimate the effect of final-state Coulomb interactions due to the assumed compact initial geometry and the neglect of finite emission times. For such an extreme scenario, we found that many-body Coulomb interactions could reduce the unperturbed values of a_2 by up to 50% for $N_C=40$. While significant, the calculated distortions cannot account for the observed variation of a_2 with N_C (by a factor of eight) when central collisions are selected by N_N.

An alternative observable expected to strongly correlate with impact parameter is the Z distribution of projectilelike fragments (PLF) observed at forward angles. Figure 4 compares PLF element distributions detected in the forward array and selected by peripheral and central cuts on N_C (solid and dotted curves, respectively) and N_N (dashed and dot-dashed

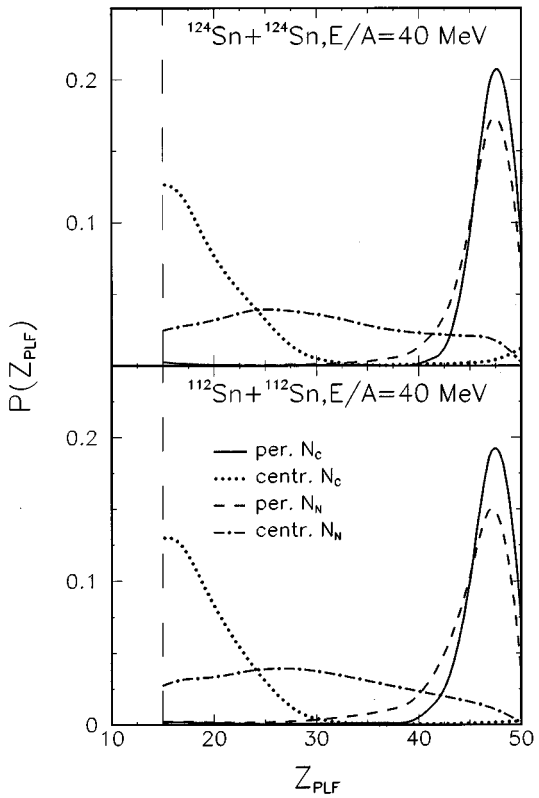

FIG. 4. Charge distributions of projectilelike fragments detected at $2.5° \leqslant \theta_{lab} \leqslant 5.4°$ for events selected by peripheral and central cuts on N_C (solid and dotted curves, respectively) or N_N (dashed and dot-dashed curves, respectively). Top and bottom panels show results for ^{124}Sn+^{124}Sn and ^{112}Sn+^{112}Sn, respectively. The long-dashed vertical line indicates the detector threshold for Z identification.

curves, respectively). In this particular case, the 2α-coincidence restriction is unnecessary; thus peripheral and central cuts represent 5% cuts of the normal event trigger yields (indicated by the dotted vertical curves in Fig. 1). The PLF distributions selected by cuts on N_C are narrower than those selected by cuts on N_N. For peripheral cuts, this difference may be less significant, but for central cuts this difference is large, suggesting much improved impact parameter selection by central cuts on N_C [28].

Qualitatively, a superior impact parameter selectivity of reaction filters based on charged-particle multiplicity may be explained in a simple participant spectator picture. Very peripheral ''binary'' collisions produce large numbers of thermal neutrons, but very few charged particles. This large thermal neutron multiplicity may present a ''background noise'' which washes out the impact parameter sensitivity for more violent collisions for which energetic neutrons and charged particles are emitted from the overlap zone between projectile and target. For charged particles, on the other hand, the background from peripheral collisions is small. Further, energetic charged particles emitted from the overlap zone are detected with higher efficiency than neutrons. The combination of these effects could lead to an improved N_C signal as soon as the overlap between projectile and target becomes appreciable.

In summary, we studied symmetric collisions of ^{112}Sn+^{112}Sn and ^{124}Sn+^{124}Sn with combined 4π-detection capability for neutrons and charged particles. We found strong evidence that better impact parameter selectivity is provided by cuts on charged particle multiplicity than by cuts on neutron multiplicity, at least over the small to mid impact-parameter range associated with significant charged particle emission [28]. This observation does not preclude the possibility that a judicious combination of charged-particle and neutron-multiplicity information might allow an additional constraint on the total dissipated energy, which is expected to fluctuate even for collisions at a fixed impact parameter. However, an experimental proof in principle for this latter possibility still needs to be established.

This work was supported by the National Science Foundation under Grant Nos. PHY-9214992, PHY-9314131, and PHY-95-28844 and by the U.S. Department of Energy under Grant Nos. DE-FG02-88ER40414 and DE-FG02-87ER40316. G.J.K. acknowledges the support of the Alexander-von-Humboldt Foundation.

[1] M. B. Tsang, G. F. Bertsch, W. G. Lynch, and M. Tohyama, Phys. Rev. Lett. **40**, 1685 (1989).

[2] J. Galin and U. Jahnke, J. Phys. G **20**, 1105 (1994).

[3] L. G. Moretto and G. J. Wozniak, Annu. Rev. Nucl. Part. Sci. **43**, 379 (1993), and references therein.

[4] J. Galin, G. Ingold, U. Jahnke, D. Hilscher, M. Lehmann, H. Rossner, and E. Schwinn, Z. Phys. A **331**, 63 (1988).

[5] M. B. Tsang, Y. D. Kim, N. Carlin, Z. Chen, R. Fox, C. K. Gelbke, W. G. Gong, W. G. Lynch, T. Murakami, T. K. Nayak, R. M. Ronningen, H. M. Xu, F. Zhu, L. Sobotka, D. Stracener, D. G. Sarantites, Z. Majka, V. Abenante, and H. Griffin, Phys. Lett. B **220**, 492 (1989).

[6] J. Péter, D. Cussol, G. Bizard, R. Brou, M. Louvel, J. P. Patry, R. Regimbart, J. C. Steckmeyer, J. P. Sullivan, B. Tamain, E. Crema, H. Doubre, K. Hagel, G. M. Jin, A. Péghaire, F. Saint-Laurent, Y. Cassagnou, R. Legrain, C. Lebrun, E. Rosato, R. McGrath, S. G. Jeong, S. M. Lee, Y. Nagashima, T. Nakagawa, M. Oshihara, J. Kasagi, and T. Motobayashi, Nucl. Phys. **A519**, 611 (1990).

[7] W. J. Llope, J. A. Conrad, C. M. Mader, G. Peilert, W. Bauer, D. Craig, E. Gualtieri, S. Hannuschke, R. A. Lacey, J. Lauret, T. Li, A. Nadasen, E. Norbeck, R. Pak, N. T. B. Stone, A. M. Vander Molen, G. D. Westfall, J. Yee, and S. J. Yennello, Phys. Rev. C **51**, 1325 (1995).

[8] L. Phair, D. R. Bowman, C. K. Gelbke, W. G. Gong, Y. D. Kim, M. A. Lisa, W. G. Lynch, G. F. Peaslee, M. B. Tsang, and F. Zhu, Nucl. Phys. **A548**, 489 (1992).

[9] L. Phair, D. R. Bowman, N. Carlin, C. K. Gelbke, W. G. Gong, Y. D. Kim, M. A. Lisa, W. G. Lynch, G. F. Peaslee, R. T. de Souza, M. B. Tsang, C. Williams, F. Zhu, N. Colonna, K.

Hanold, M. A. McMahan, and G. J. Wozniak, Nucl. Phys. **A564**, 453 (1993).

[10] D. X. Jiang, H. Doubre, J. Galin, D. Guerreau, E. Piasecki, J. Pouthas, A. Sokolov, B. Cramer, G. Ingold, U. Jahnke, E. Schwinn, J. L. Charvet, J. Frehaut, B. Lott, C. Magnago, M. Morjean, Y. Patin, Y. Pranal, J. L. Uzureau, B. Gatty, and D. Jacquet, Nucl. Phys. **A503**, 560 (1989).

[11] R. T. de Souza, L. Phair, D. R. Bowman, N. Carlin, C. K. Gelbke, W. G. Gong, Y. D. Kim, M. A. Lisa, W. G. Lynch, G. F. Peaslee, M. B. Tsang, H. M. Xu, F. Zhu, and W. A. Friedman, Phys. Lett. B **268**, 6 (1991).

[12] B. Lott, S. P. Baldwin, B. M. Szabo, B. M. Quednau, W. U. Schröder, J. T̃oke, L. G. Sobotka, J. Barreto, R. J. Charity, D. G. Sarantites, D. W. Stracener, and T. T. de Souza, Phys. Rev. Lett. **68**, 3141 (1992).

[13] J. T̃oke, B. Lott, S. P. Baldwin, B. M. Quednau, W. U. Schröder, L. G. Sobotka, J. Barreto, R. J. Charity, D. G. Sarantites, D. W. Stracener, and R. T. de Souza, Phys. Rev. Lett. **75**, 2920 (1995.)

[14] M. D'Agostino, G. J. Kunde, P. M. Milazzo, J. D. Dinius, M. Bruno, N. Colonna, M. L. Fiandri, C. K. Gelbke, T. Glasmacher, F. Gramegna, D. O. Handzy, W. C. Hsi, M. Huang, M. A. Lisa, W. G. Lynch, P. F. Mastinu, C. P. Montoya, A. Moroni, G. F. Peaslee, L. Phair, R. Rui, C. Schwarz, M. B. Tsang, G. Vannini, and C. Williams, Phys. Rev. Lett. **75**, 4373 (1995).l

[15] M. D'Agostino, A. S. Botvina, P. M. Milazzo, M. Bruno, G. J. Kunde, D. R. Bowman, L. Celano, N. Colonna, J. D. Dinius, A. Ferrero, M. L. Fiandri, C. K. Gelbke, T. Glasmacher, F. Gramegna, D. O. Handzy, D. Horn, W. C. Hsi, M. Huang, I. Iori, M. A. Lisa, W. G. Lynch, L. Manduci, G. V. Margagliotti, P. F. Mastinu, I. N. Mishustin, C. P. Montoya, A. Moroni, G. F. Peaslee, L. Phair, R. Rui, C. Schwarz, M. B. Tsang, G. Vannini, and C. Williams, Phys. Lett. B **371**, 175 (1996).

[16] G. J. Kunde, S. Gaff, C. K. Gelbke, T. Glasmacher, M. J. Huang, R. Lemmon, W. G. Lynch, L. Manduci, L. Martin, M. B. Tsang, W. A. Friedman, J. Dempsey, R. J. Charity, L. G. Sobotka, D. K. Agnihotri, B. Djerroud, W. U. Schröder, W. Skulski, J. T̃oke, and K. Wyrozebski, Phys. Rev. Lett. **77**, 2897 (1996).

[17] W. U. Schröder, University of Rochester Report DOE/ER/79048-1, 1995 (unpublished).

[18] R. T. de Souza, N. Carlin, Y. D. Kim, J. Ottarson, L. Phair, D. R. Bowman, C. K. Gelbke, W. G. Gong, W. G. Lynch, R. A. Pelak, T. Peterson, G. Poggi, M. B. Tsang, and H. M. Xu, Nucl. Instrum. Methods Phys. Res. A **295**, 109 (1990).

[19] M. B. Tsang, W. C. Hsi, W. G. Lynch, D. R. Bowman, C. K. Gelbke, M. A. Lisa, G. F. Peaslee, G. J. Kunde, M. L. Begemann-Blaich, T. Hofmann, J. Hubele, J. Kempter, P. Kreutz, W. D. Kunze, V. Lindenstruth, U. Lynen, M. Mang, W. F. J. Müller, M. Neumann, B. Ocker, C. A. Ogilvie, J. Pochodzalla, F. Rosenberger, H. Sann, A. Schüttauf, V. Serfling, J. Stroth, W. Trautmannn, A. Tucholski, A. Wörner, E. Zude, B. Zwieglinski, S. Aiello, G. Immé, V. Pappalardo, G. Raciti, R. J. Charity, L. G. Sobotka, I. Iori, A. Moroni, R. Scardoni, A. Ferrero, W. Seidel, Th. Blaich, L. Stuttge, A. Cosmo, W. A. Friedman, and G. Peilert, Phys. Rev. Lett. **71**, 1502 (1993).

[20] Neutron absorption in the material of the Miniball is estimated to be on the order of a few percent and has little effect on the performance of the SuperBall.

[21] C. B. Chitwood, D. J. Fields, C. K. Gelbke, D. R. Klesch, W. G. Lynch, M. B. Tsang, T. C. Awes, R. L. Ferguson, F. E. Obenshain, F. Plasil, R. L. Robinson, and G. R. Young, Phys. Rev. C **34**, 858 (1986).

[22] M. B. Tsang, R. T. de Souza, Y. D. Kim, D. R. Bowman, N. Carlin, C. K. Gelbke, W. G. Gong, W. G. Lynch, L. Phair, and F. Zhu, Phys. Rev. C **44**, 2065 (1991).

[23] L. Phair, L. G. Moretto, G. J. Wozniak, R. T. de Souza, D. R. Bowman, N. Carlin, C. K. Gelbke, W. G. Gong, Y. D. Kim, M. A. Lisa, W. G. Lynch, G. F. Peaslee, M. B. Tsang, and F. Zhu, Phys. Rev. Lett. **77**, 822 (1996).

[24] R. Lacey, A. Elmaani, J. Lauret, T. Li, W. Bauer, D. Craig, M. Cronqvist. E. Gualtieri, S. Hannuschke, T. Reposeur, A. Vander Molen, G. D. Westfall, W. K. Wilson, J. S. Winfield, J. Yee, S. Yennello, A. Nadasen, R. S. Tickle, and E. Norbeck, Phys. Rev. Lett. **70**, 1224 (1993).

[25] M. A. Lisa, W. G. Gong, C. K. Gelbke, and W. G. Lynch, Phys. Rev. C **44**, 2865 (1991).

[26] Consistent with statistical expectations [21], the ''V''-shaped azimuthal 2α correlation becomes more pronounced for more energetic particles, see, e.g., M. B. Tsang *et al.*, Phys. Rev. C **47**, 2717 (1993). Suppression of low-energy α particles enhance the ''signal,'' but the inclusion of lower-energy α particles does not alter our conclusions.

[27] Azimuthal correlations become strongly attenuated [9] for impact parameters $b \rightarrow 0$, because near-central collisions correspond to smaller entrance channel angular momenta and to higher energy depositions (or temperatures). Both effects attenuate the ''V''-shaped azimuthal correlations [21,23].

[28] For peripheral ''binary'' collisions in which very few or no charges particles are emitted, event selection with event filters based upon N_N is superior. These less violent collisions are, however, strongly suppressed by the event trigger employed in this experiment.

[29] The functional, Eq. (2), was chosen to be consistent with previous work [9,23,24]. While our fits with this formula are of comparable quality as those in previous work, better fits can be obtained by including higher order terms. The use of alternative measures of the azimuthal anisotropies, e.g., $[Y(0°) + Y(180°)]/2Y(90°\mathrm{E})$, does not alter the conclusions of this paper—as is readily seen from Fig. 2.

[30] R. Popescu, C. K. Gelbke, and T. Glasmacher, Phys. Rev. C **54**, 796 (1996).